Geology, Geodynamics, and Atmospheric Electricity

Geology, Geodynamics, and Atmospheric Electricity

By

Vladimir N. Shuleikin

Cambridge
Scholars
Publishing

Geology, Geodynamics, and Atmospheric Electricity

By Vladimir N. Shuleikin

Reviewers:
Dmitrievsky A. N., Academician of the Russian Academy of Sciences;
Nikolaev A. V., Full Member of the Russian Academy of Sciences

This book first published 2020

Cambridge Scholars Publishing

Lady Stephenson Library, Newcastle upon Tyne, NE6 2PA, UK

British Library Cataloguing in Publication Data
A catalogue record for this book is available from the British Library

ISBN (10): 1-5275-4442-7
ISBN (13): 978-1-5275-4442-0

This research was performed under the auspices of the Oil and Gas Research Institute, Russian Academy of Sciences (3 Gubkina Street, 119333, Moscow, Russia) and was approved for publication by the Academic Council of the Institute.

In memory of my first teachers:
My grandfather, Alexander Kondratievich Kondratiev,
and my father, Nikolai Mikhailovich Shuleikin

TABLE OF CONTENTS

Preface ix

Introduction 1

Chapter 1 5
Atmospheric Electricity and the Physics of the Earth
1.1. The History of Observation and Equipment 6
1.2. Model of the Relationships between Hydrogen, Methane, Radon, and Elements of Surface Atmospheric Electricity 18
1.3. AEF Sensitivity to Changes in the Density of Hydrogen and Methane 31
1.4. References to Chapter 1 41

Chapter 2 46
Space Charge of Surface Air: The Electrode Effect
2.1. Surface Air Ionizers 47
2.2. Radon Transfer to Surface Soil Layers and the Atmosphere 56
2.3. The Electrode Effect in the Atmospheric Surface Layer 64
2.4. References to Chapter 2 70

Chapter 3 74
Atmospheric Electricity above Geological Heterogeneities
3.1. Surface Atmospheric Electricity above Fault Zones and Areas of Geological Deconsolidation 75
3.2. An Ore Body and an Oil Deposit 85
3.3. Atmospheric Electricity above a Gas Deposit 93
3.4. References to Chapter 3 102

Chapter 4 106
Geodynamic Processes and Surface Atmospheric Electricity
4.1. Complex Hydrogen-Radon and Atmospheric-Electrical Observations of a Landslide 107
4.2. Experimental Verification of Causal Relationships between the Microseismic, Hydrogeological, and Atmospheric-Electrical Fields 123
4.3. Geology, Geodynamics, and Thunderstorm Activity 133
4.4. References to Chapter 4 143

Conclusion 148

PREFACE

Atmospheric electricity is a research problem in geophysics that consistently attracts the attention of researchers to a variety of phenomena and processes. These involve, directly or indirectly, natural and man-made sources and complex systems taking place in the various shells of the Earth: the lithosphere, the hydrosphere, and the atmosphere. With high energy saturation (from thunderstorm activity) and the complexity of the distribution of electrical, magnetic, and mechanical properties, the Earth's crust, the surface layer of the troposphere adjoining it, the stratosphere, and the ionosphere constantly exhibit unpredictable behavior that has not yet been explained by modern science. On the one hand, the role of electrical phenomena in lithospheric processes associated with the generation of earthquake foci and seismicity is not entirely clear. On the other hand, there is no absolutely clear explanation as to the influence of earthquake generation processes in the formation of anomalous electrical phenomena in the atmosphere. The same can be said about other catastrophic phenomena, such as typhoons, tornadoes, and linear cloud formations over fault zones, which are especially noticeable shortly before seismic events. Similar anomalous phenomena accompanying robust man-made processes include underground nuclear explosions, to which lightning discharges in the atmosphere at the surface level should be added.

At first sight, it is logical to consider the electrical phenomena observed in the atmosphere to be a continuation of telluric processes that take irregular forms and expand their role in the surface atmosphere during the period preceding cataclysmic Earth events. However, this approach cannot be explained from the position of physics. It cannot be assumed that, even in the case of small-focus earthquakes, electric fields generated in the Earth will be discharged through the atmosphere. Even assuming the formation of local anomalous charges, with a linear or circular current source in the area of the hypocenter, their electric fields will be shielded by kilometer-thick layers of sedimentary rock cover, the conductivity of which is many orders of magnitude higher than that of atmospheric air.

For more than 35 years, the author of this monograph has been engaged in experimental study into the connections between geological heterogeneities and processes in the Earth's crust and the elements of surface atmospheric electricity. This work, as well as the work of most geophysicists-researchers in the field of atmospheric electricity, are associated with the forecasting of earthquakes. Preliminary surveys were undertaken on a vibrational testing ground to identify the interrelations of elements of surface atmospheric electricity, which have a powerful effect on the geological environment, and changes in hydrogeological and geochemical fields in the zone of artificial microvibrations.

The classical theory of atmospheric electricity and the radon mechanism for generating the space charge of the surface layer of air was taken as the theoretical grounds of the interactions being studied. Based on numerous field observations, a representational model of the relationships between hydrogen, methane, radon, and surface atmospheric electricity elements was developed. Bubbles of two volatile gases carry radon into the surface atmosphere where, as a result of ionization, light ions are formed that provide polar conductivity in the air. The combination of light ions with neutral condensation nuclei creates heavy ions, which are primarily responsible for the atmospheric electric field. To put it differently, the local space charge of the surface atmosphere is determined by content of the parent substance—radium—at depths of the first few meters below the Earth's surface and sub-vertical volatile gas flux density. This means that any geological anomalies and geodynamic processes that can change hydrogen and methane flux density will inevitably cause changes in the elements relevant to surface atmospheric electricity.

In 1988, the Interdepartmental Geophysical Committee of the Presidium of the Russian Academy of Sciences established a commission—the Global Electrical Circuit Project—for the purpose of developing and adapting research into interactions in the complex lithosphere-atmosphere-ionosphere system. The field observation materials provided in this monograph, and their interpretation, will be of interest in understanding the first stage of these interactions and the relationships between geology, geodynamics, and surface atmospheric electricity.

This book is unconventional in its content and methodological approaches to the study of electrical processes in identifying their relationships with the processes of different physical origins. The results of the complex atmospheric-electrical, seismic, hydrogeological,

and geochemical observations presented in this monograph unequivocally indicate the interrelations of the above-listed fields. Groundwater-level dynamics regulate ionizer injection into the atmosphere, while seismic effects aggravate this regulation. Any municipal water intake can increase the atmospheric electric field by an order of magnitude in the depression funnel zone. The efficiency of seismic acceleration in the process increases with a period of microvibrations.

The results of atmospheric-electrical and hydrogen-radon monitoring are all of applied interest in research into: fault zones; ore bodies; basement rock areas; oil fields and the dynamics of their development; the process of combustible gas dispersion in an underground gas storage reservoir bed; and the stress-state of a landslide, the movement of which can be provoked by the laying of a pipeline.

In academic courses on atmospheric electricity, changes in the electrical characteristics of the surface air layer are associated exclusively with the dynamics of the meteorological situation. The data in this book enhances our understanding of the physical origin of this phenomenon. In stable meteorological conditions, changes in the electrical characteristics of the surface air layer are determined exclusively by the geological and geodynamic features of the environment.

The author of this monograph solves here a number of unconventional problems and, at the same time, discovers new effects and antimonies, the explanation of which will be marked by advances in geophysical science in years to come.

Academician A. N. Dmitrievsky

INTRODUCTION

In the mid-eighteenth century, Benjamin Franklin suggested an experiment using a kite flown into a thunderstorm cloud. The investigation was conducted independently by T. Delibard and B. Franklin and completed with the creation of the lightning conductor. At the same time, after experiments on a "thunder machine," Mikhail Lomonosov formulated the first hypothesis on the charging of thunderstorm clouds. Today's research suggests the existence of a multistage global electrical circuit connecting the Earth's shells and the atmosphere in an integrated system. The establishment of relationships between parallel processes in different Earth shells highlights the problem of the global electrical chain. The phenomena of interest in studying the global electrical chain are at the planetary-spatial scale and require the use of rockets, ionospheric balloons, and aircraft; and the taking of measurements in space, at ground level, and in the lithosphere.

In 1890, the primary experimental results on disturbances of the electric potential in the atmosphere—the atmospheric electric field—before, during, and after seismic events were obtained at the Imperial Meteorological Observatory in Tokyo. Perturbations of the field recorded with clear weather conditions before the 1926 earthquake in Kyrgyzstan were named the "Electric Storm." In the mid-twentieth century, extensive field material on abnormal variations of the atmospheric electric field before seismic events was obtained at the Gharm Forecasting Test Site of the Institute of Earth Physics, RAS. Up to the present day, in the scientific literature, one can find only a few works that describe such field anomalies during drastic changes in the seismic mode. As per accepted classification, these perturbations relate to short-term precursors, are bipolar, and are several times larger in magnitude than the general background signal level. Their development can take from tens of minutes to hours before an earthquake.

P. Tverskoi and J. Chalmers, the founders of the surface atmospheric electricity theory, have pointed to radon as the origin of the surface charge of atmospheric surface air. The ionization process forms a pair of light ions that determine the polar

conductivities of the air. The combination of light ions with neutral condensation nuclei creates heavy ions, which are primarily responsible for the formation of the atmospheric electric field.

The negative charge of the Earth and the presence of positive and negative ions in the surface atmosphere inevitably led researchers to discover the electrode effect. At first, the problem was addressed by approximating the presence of light ions in air at the Earth's surface. Such estimates did not correspond to the actual atmospheric situation, where heavy ion density is almost an order of magnitude higher than light ion density. However, this does not contradict the physics of the atmospheric situation, which sees the presence of positive and negative ions of comparable concentrations in surface air.

In studying the relationship of the atmospheric electric field to altitude, it was immediately possible to distinguish two cases: the classical electrode effect and the reverse electrode effect. In the first case, with a low ionization rate—a low concentration of emitted soil radon—the electrical field smoothly decreases with the height of the relatively negatively charged electrode and reaches a background level determined solely by the space charge. At a high ionization rate—a high radon concentration—a negative space charge layer forms above the ground; after a particular height the field then decreases below the background level, the yield of which follows a curve that describes the measurements of field values if they were to be plotted on a graph.

The calculation of the classical and reverse electrode effects led to an understanding of the bipolar nature of changes in the atmospheric electric field before earthquakes. If the measurements were carried out in the compression zone where ionizer emission was minimized, the measuring device recorded abnormally high fields. In the extension zone, the release of soil radon into the atmosphere reached its maximum. Here, at the Earth's surface, a thick layer of negative space charge was formed and measurements of the atmospheric electric field showed the formation of abnormally low negative fields.

The mechanism of soil radon transport into the near-surface atmosphere remained an open question. The high molecular weight of the ionizer, Rn^{222}, precluded the possibility of its isolated sub-vertical migration. For a long time, we believed that bubbles of all the volatile gases in soil air acted as ionizer carriers, bringing radon to the surface. However, radon detection at altitudes of several kilometers during the taking of measurements from an aircraft has

suggested a limited density of the carrier gases. Radon efflux to altitudes of several kilometer could only be performed by gases whose density is less than the density of atmospheric air. These gases potentially also include four ingredients of soil air: hydrogen, helium, methane, and water vapor. Helium, like radon, belongs to the category of inert gases and the capture of one inert gas by a bubble of another inert gas is impossible. The evaporation process takes place in a thin surface layer of the ground, where the radon soil concentration is almost equal to its atmospheric level. Even if water vapor participated in radon transport, the contribution of the ionizer transported by water vapor to the total radon content in the atmosphere would be minimal. Additional experimentation has confirmed this conclusion.

Following this logic, one can state that the soil-to-atmosphere air exchange determines the space charge dynamics of the surface air at the point of observation. The half-life of radon is 3.8 days, which suggests that the emanated gas must enter the atmosphere from shallow depths. This is because as over a period of three half-lives, its concentration decreases by almost an order of magnitude. All this means that the emitted soil radon is only a mediator, which opens up the possibility of tracking the density of sub-vertical hydrogen and methane fluxes through measuring local values of polar conductivities and the atmospheric electric field.

In fracture zones, intensification of the soil-to-atmosphere air exchange is observed. Excessive methane concentrations are present in oil field plumes and electrochemical processes in the caps of ore bodies increase the hydrogen concentration in soil air.

Recording of the abnormal electrical characteristics of surface air before seismic events is somewhat random, as the researcher must be in the right place at the right time. Measurements of the atmospheric electric field and polar air conductivities above geological anomalies and in geodynamic process zones can be performed in a targeted manner. The results of these studies and their analysis form the basis of this monograph.

The author considers it a pleasant duty to express his deep gratitude to Alexei Vsevolodovich Nikolaev, the Corresponding Member of the Russian Academy of Sciences, whose support allowed me to carry out research in Belarus and Central Asia and the Academician, Anatoly Nikolayevich Dmitrievsky, who is the moderator of research into hydrocarbon accumulations. I also wish to thank my colleagues and friends: Reznichenko Alexander

Pavlovich, Barabanov Vyacheslav Leonidovich, and Gufeld Iosif Lippovich for their help in carrying out fieldwork; Professor Georgy Georgievich Shchukin, the co-author of many of my articles. I make a deep bow to: Ilya Moiseevich Imyanitov, Dr. Sci. in Physics and Mathematics; Yakov Mikhailovich Schwartz, Ph.D. in Physics and Mathematics; Georgy Ivanovich Voitov, Dr. Sci. in Geology and Mineralogy; Professor Dmitry Nikolayevich Chetaev; Alexey Mikhailovich Polykarpov, Ph.D. in Physics and Mathematics who has passed on and whose help in performing tests and fieldwork and interpreting the results has been invaluable.

CHAPTER 1

ATMOSPHERIC ELECTRICITY AND THE PHYSICS OF THE EARTH

In the mid-eighteenth century, the practical study of lightning electricity started in both Russia and the USA almost simultaneously. In 1745, Mikhail Lomonosov and Georg Richmann designed the first electrical-type instrument—the 'electric indicator.' This electric indicator differed from the famous electroscope in its use of a wooden quadrant with a scale, which allowed the quantitative assessment of the deflection of a linen thread from the vertical plane. This innovation allowed the measurement of a "higher or lower electricity level."

A wire connected the electric indicator to a metal rod on the laboratory roof. The "thunder machine" showed that electricity existed in the atmosphere, even in fair weather.

In 1750, B. Franklin suggested an experiment that used a kite flown into a thunderstorm cloud. On May 10, 1752, the French physicist Thomas-François Dalibard carried out the same investigation. The work by Benjamin Franklin logically resulted in the design of a lightning conductor. According to B. Franklin, the lightning conductor "…either prevents lightning discharge from a cloud or, already at the discharge, deflects the lightning to the ground without any detrimental effect to a building…." In 1760, B. Franklin installed the first lightning conductor on the house of the tradesman Benjamin West in Philadelphia.

Since the early nineteenth century, the interest of researchers in studying thunderstorm electricity has subsided a bit and the focus has been on the study of "fair weather" electricity. At the end of the 1800s, Japanese researchers showed the presence of abnormal changes in the potential of the atmosphere before, during, and after earthquakes. Up to the present day, one can find several (20–30) publications on changes in the atmospheric electric field before seismic events in the scientific literature.

The discovery of the radon mechanism of surface space charge generation provided the foundation for the modelling of the relationships between gas and electric fields in the ground and the atmosphere. Bubbles of hydrogen and methane transport soil radon to the surface atmosphere where, in the ionization cycle, light ions form. These are responsible for the polar conductivity of the air. The aggregation of light ions with neutral condensation nuclei causes the formation of heavy ions, which are primarily responsible for the atmospheric electric field (AEF).

1.1. The History of Observation and Equipment

Published results of instrumental observations indicating the appearance of unusual perturbations of the atmospheric electric field (AEF) before an earthquake are very few. In the late nineteenth century, the Imperial Meteorological Observatory in Tokyo implemented annual monitoring of the atmospheric potential. Nine times out of ten, strong earthquakes with foci as far as 100 km from Tokyo were seen to induce anomalous perturbations in the field [1].

Before an earthquake of magnitude M = 4.5 occurred on August 1, 1924, in Kyrgyzstan, disturbances of the AEF of a very complex shape were recorded at a distance of about 150 km from the epicenter in clear weather:

- 5 hours before the seismic event, a decrease in the signal level began;
- 4 hours before, intense discharges and charges of the electrometer at a frequency of 1.0–1.5 Hz began;
- at the same time, the maximum field values reached 1,000 V/m [2].

In 1946, before the Chatkal Earthquake, and in 1949, before earthquakes in Dushanbe and Obi-Gharm, similar effects were observed [3]. In the cases considered, the sign of the recorded parameter also changed.

Five hours before the Tashkent Earthquake, with a magnitude M = 5.3, took place on April 26, 1960, a change in the vector of the atmospheric electric field was recorded in the epicentral zone [4]. The meteorological situation in the observation area on the eve of the earthquake was turbulent; it stabilized only a few hours before the seismic event. Anomalous AEF perturbations were also recorded

before several of the most powerful aftershocks. However, in most cases, no noticeable changes in the field before most of the aftershocks were observed.

Immediately after the catastrophic Khait Earthquake occurred on June 10, 1949, monitoring and AEF measurements 50 km from the epicenter were initiated by the Gharm Expedition of the Schmidt Institute of Earth Physics. In 22 out of 23 cases, 1.5–2.0 hours before the strongest aftershocks, with M = 5–6 at the observation point, an increase in the signal of ~100 V/m was observed. Over the summer season of 1950–51, in the same area, the atmospheric electric field was continuously recorded at five points. Perturbations of the AEF, similar in form to those before local seismic events of M = 5–6 were successfully recorded [5].

Up to today, the field observations obtained at the Gharm Test Range of the Schmidt Institute of Earth Physics represent the most significant source of information on abnormal AEF precursors before seismic events [6]. Modern retrograde analysis of the results has allowed the rejection of some of the recorded anomalous field changes, as they were associated exclusively with current changes in the meteorological situation [7]. However, even taking into account the current level of scientific knowledge and instrument capability, it is necessary to pay tribute to the high professionalism of those experts who developed unique experimental material in the middle of the past century.

In 1977, AEF disturbances were recorded at the Gharm Test Range at three observation points 1 to 2.5 days before a K = 13 earthquake and at epicentral distances of 20–35 km. The perturbations took the form of distinct oscillations with a period of 6–10 minutes [8].

At an observation station in China [9], before earthquakes of M = 4.6–6.1, anomalous decays of AEF were observed at epicentral distances of 100–250 km. Perturbations occurred at time intervals ranging from several days to one month before a seismic event and reached 500–950 V/m. During periods of seismic calm, such disturbances were not observed.

Further observations over the past 12 years have confirmed the reliability and stability of such manifestations of AEF anomalies [10, 11]. Following analysis of the results of observation, certain regularities of earthquake precursors were established based on AEF monitoring data. Their geographical features were highlighted and theoretical ideas were developed that satisfactorily explained

the nature of the anomalies observed [12, 13]. Similar decreases in AEF before an earthquake are discussed in [14].

The field changed its sign at an epicentral distance of 18 km, six hours before an earthquake of magnitude M = 3.5 in California. About a day before another seismic event of the same energy, with calm weather conditions, oscillations with a total duration of about four hours were recorded at two points with epicentral distances of 8 km and 20 km. At a position 50 km from the epicenter, no anomalous perturbations of the AEF were detected [15]. Fluctuations in AEF intensity before an earthquake, class $K = 11$, are described in [16].

Convincing results on variation in AEF before earthquakes are presented in [17, 18]. Unfortunately, these studies only provide a concise (less than a day) series of observations, which do not allow us to assess the origin of background field variations before and after seismic events. Description of the meteorological situation is limited to mentioning the calmness of the weather at the observation point and we cannot speak confidently about the tectonic origin of the recorded anomalies.

The space charge of air at the Earth's surface owes its origin to ionization from emitted soil radon [19–22]. In the summer of 1914, this effect was used when prospecting for radioactive ores by the Moscow Radium Expedition in Fergana, Uzbekistan [23]. In 1919, S. Kurbatov performed laboratory studies on the ionizing radiation of rocks sampled from the Yulin Mine near Minusinsk, Krasnoyarsk Krai, Russia. In 1920, using these lab results, he succeeded in detecting a deposit of radioactive ores located 12–13 km southeast of the Yulin Mine.

In performing field observations, classical measuring devices are used to record polar conductivities (PCs) and AEF—an aspiration capacitor unit combined with a field mill have been used around the world to take atmospheric-electrical measurements for decades. Let us turn to the refinement of the technique of using these devices in the field.

To reduce the sensitivity of the PC sensor to an external wind load, in some cases, a block of aspiration condensers was mounted vertically above a ~20-liter pit and the "soil air" was purged directly through the condensers [24]. When specialized observations are performed from a vehicle, a set of aspiration condensers is placed on the back seat; the air is purged through an open window; and the machine is oriented perpendicular to the wind direction.

Until the mid-1990s, the signal was recorded using a two-channel analog data recorder, and later on by a personal computer. In the latter case, in the presence of noticeable variations of signals relative to the average level, the correlation coefficient between them was calculated at once. When the correlation coefficient was below 0.8, the measurement was repeated.

In the initial experiments measuring the AEF profile, the field mill was placed on the ground at each observation picket [25]. Sometimes, towing it on a sled-trailer behind a motor vehicle led to noise contamination of the signal due to the accumulation of dust. The best way to install the measuring device is in the roof hatch of a car. Measurements were always carried out in fair weather conditions [26–28]. Each controlled profile was passed at least twice, Figure 1.1.1.

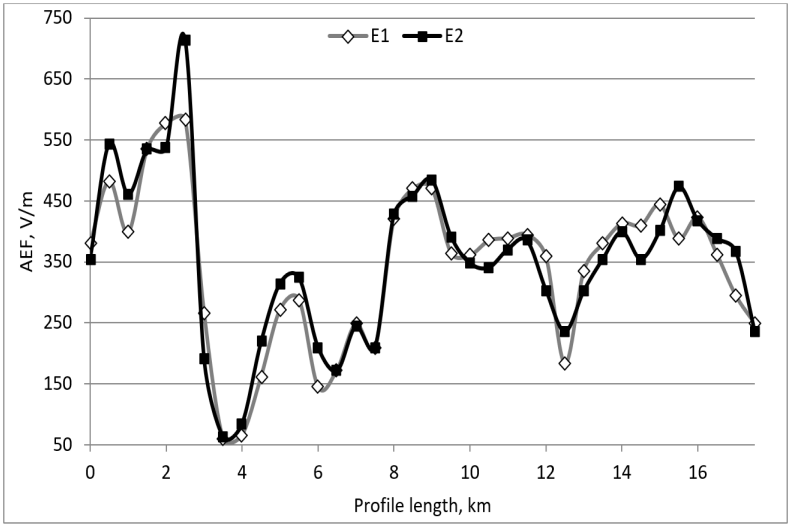

Figure 1.1.1: An example of recording AEF for a double-pass, E1 & E2, profile length of 17.5 km.

Due to the limited demand for AEF sensors, this device has never been serially manufactured. The most extensive series of the Pole-2 device was designed and manufactured at the Experimental and Production Workshops of A. I. Voeykov Main Geophysical Observatory. For many years, AEF sensors have been in operation at the Voeykovo settlement and at several meteorological stations,

including: Verkhnee Dubrovo; Dusheti; Irkutsk, Yuzhno-Sakhalinsk; Karadag, Kyiv; Murmansk; and Odesa [29]. For mobile AEF observations, a gradient measuring device from the same manufacturer, designed to be powered by an autonomous 12 V power supply, was used.

Before developing a measuring device for a regime of forecast observations at five pickets at a landfill site in Tajikistan, based on observations in the Tiksi Bay [30], AEF and the air-earth current were studied. The measurements were carried out using a sensor grid [31] at a height of 1 m above the ground on four insulated pillars. A grid of 100 m² area and a cell size of 0.1 m × 0.1 m was installed. Figure 1.1.2 shows the air-earth current variations recorded in fair weather conditions, including still air and zero cloud cover. The AEF was simultaneously recorded.

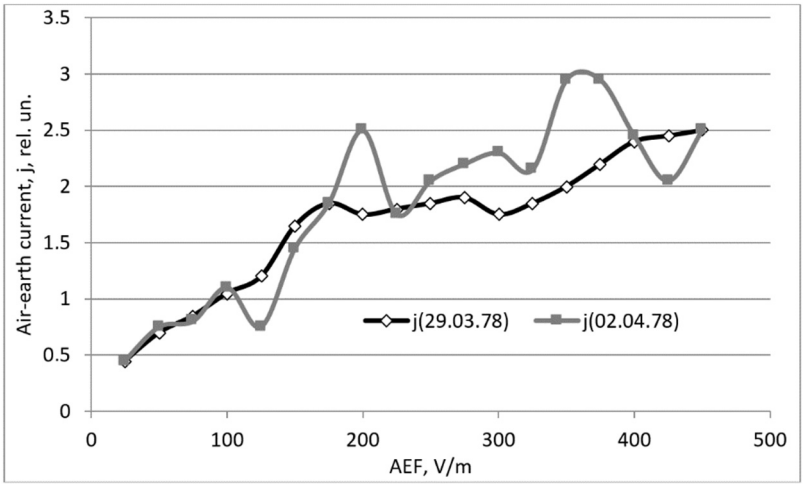

Figure 1.1.2: Non-linear origin of Ohm's law in the atmosphere with measurements at Tiksi Bay.

Formal mathematical evaluation allows us to say that in fields of up to 100 V/m, the accuracy of the linear field and current approximation is D ~0.95–0.98 and the scatter of the reduction coefficient, k, is below 2 %; up to 200 V/m—D ~ 0.85–0.95, k ~(2–9) %; up to 300 V/m—D ~0.85, k ~(35–66) %; and up to 400 V/m—D ~0.85, k ~(54–104) %. In fields of over 200 V/m, however, the linearity of Ohm's law in the atmosphere is violated.

Taking into account the abnormal changes in the AEF recorded before seismic events (see above) and deviations from Ohm's law in fields above 200 V/m, the air-earth current was chosen as a control parameter at observation pickets in Tajikistan. Disadvantages of the grid sensor included: low noise immunity where convection currents were concerned; vortex movements of dust charge formations; low technological capability at the test installation; and long-term operation of the collecting element. Continuous operation of the current sensor in Central Asia required us to solve the problem of ensuring noise immunity of the measuring device to interference from the surface layers of dust that formed up to a thickness of several decimeters.

A single-wire antenna was used as the basis of the measuring device [19, 32, 33]. To minimize near-surface interference, the antenna height was increased to 5–6 m. At the same time, this increase improved the technical capability of the sensor, as it eliminated the possibility of the collecting element being disconnected, for example, by vehicles passing over it. Furthermore, a second, additional collecting element was added to the measuring circuit. This element was located on the same plane as the main element, in parallel with it and the Earth's surface. The main and additional antennas were separated by a distance of an order of magnitude smaller than their installation heights: $\Delta H = H(A1) - H(A2)$. At the same time, the signal difference at the output of the main and additional antennas minimized common mode interferences from convection currents and near-surface dust formations.

Differential antenna operation was repeatedly verified by comparison with field results and conductivity measurements at the Voeykovo and Borok Observatories [34]. Figure 1.1.3 shows synchronous records of the air-earth current and AEF. The extremely high reliability of the field mill and differential antenna operation is illustrated by a 31-hour recording period that was obtained under extremely unfavorable weather conditions. The collecting elements of the differential antenna of 80 meters in length were installed on nylon extensions and with fluoroplastic insulators between the roof of the laboratory building and the mast, which was installed 100 m away from the building. The height of suspension of the upper collecting element of the passive differential antenna was $H(A1) = 8$ meters with a spacing of 0.6 m.

The Pole-2 field mill was installed on the roof. For the convenience of data comparison, all the records in Figure 1.1.3 are

given in relative units. The AEF sensor was calibrated in absolute units: a 300 V/m field corresponds to 10 rel. units of the scale used.

The correlation coefficients between parameters for 31 hours of continuous observation equal: *k*[AEF; *j*(dif.ant.)] = 0.8; *k*[AEF; *j*(grid)] = 0.6; *k*[*j*(dif.ant.); *j*(grid)] = 0.62. On a purely formal basis, records obtained by a differential passive antenna are closely related to changes in the atmospheric electric field.

The extremely flat pattern of recordings from the "grid" in the period of 5 to 26 hours and the signal minimum at the 27th hour of observation is doubtful. At the AEF and *j*(dif.ant.) channels, this minimum occurred one hour earlier, when snowfall began to decline. The recorded delay can, most likely, be attributed to leaks from the "grid" installation masts. Joint tests of measuring devices have shown that a field mill and a differential antenna comprise the meteorological sensors with the lowest noise.

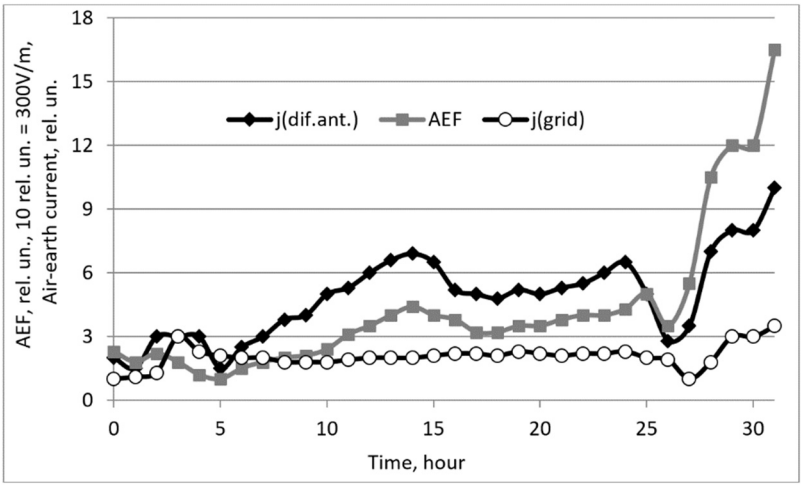

Figure 1.1.3: Synchronous recordings from the differential antenna *j*(dif.ant.), the field mill—AEF, and the gauge of "grid" type *j*(grid), obtained between 08h 00m 02/01/87 and 15h 00m 02/02/87. 31 hours of continuous recording under extremely adverse meteorological conditions: hours 2–4 fog; hours 10–15 strong wind; hour 26 snow showers; hours 29–31 strong wind, clear.

Tests of the differential antenna were carried out at one of the stations of a forecast test range in Tajikistan. Figure 1.1.4 shows nine eight-minute signal recordings using a single-wire and

differential antennas with different installation heights and separations. The upper graph presents the optimal variant of installation height and separation of the differential antenna. If consecutive recordings from single-wire antennas—only the upper one H(A1) with the lower one removed or, vice versa, H(A2)—are characterized by a 40–80 % signal scatter, then recordings from the differential antenna (dif.ant.) have a separation of ΔH = 0.57 m, as expected this is much more stable and characterized by scattering with a level of 16 % in total.

The situation is somewhat worse for the case where the suspension height of the additional antenna was reduced to H(A2) = 4.15 m, and the separation was increased to ΔH = 0.82 m. The signal scatter of the single-wire antennas H(A1) and H(A2) increased by 30–77 %. At the same time, the effect of differential reception and signal amplification also deteriorated and the signal scatter during the eight-minute recording increased to 19 %.

The effect on differential reception and amplification of the signal of the drop in elevation can be seen in the lower graph in Figure 1.1.4, where the installation height of the additional antenna was H(A2) = 3.44 m and the separation was ΔH = 1.53 m. The signal scatter from the upper, H(A1), and lower, H(A2), single-wire antennas was 31–86%; while from the differential antenna it was 24 %.

The control measurements performed show that the measuring device developed significantly reduces the noise component of the signal, which is associated with convection currents, dust surface charges, and dust charge transfer. With the help of a differential antenna, several anomalous air-earth current variations were recorded; these are described below.

Since the mid-1990s, atmospheric-electrical measurements have always been performed in conjunction with observations of soil-air hydrogen and radon. In all the complex measurements described below, a radon volumetric activity sensor, RGA-01, was used, which was able to operate in an ambient temperature range of +5 °C to + 50 °C. The relative error of a single count was 30 % when operating in the range of 10^{-2}–10^{3} Bq/l. In the course of observation, each soil air sample from the sampling well at the picket was analyzed four times.

The 15-year experience of operating the measuring device, especially in temperatures of 30 °C or higher, led to the development of an optimal technique for taking four rapid and consecutive radon readings from samples of the soil air and the atmospheric air. A

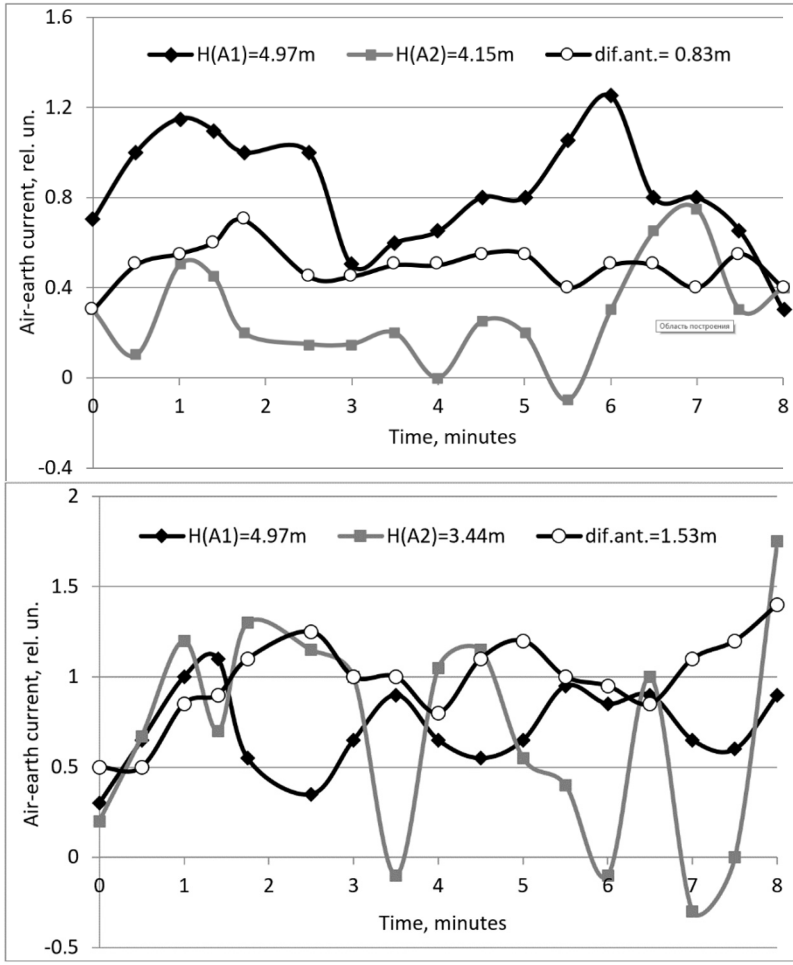

Figure 1.1.4: Examples of 8-minute recordings of the air-earth current signal recorded by single-wire and differential passive antennas with different installation heights.

minimal loss of time and accuracy at the observation picket can be achieved when the first count is read at a 200 s time interval, and the next three counts are read at 20 s intervals. The reason for this is that there is a significant difference in the temperature of the soil air and the atmospheric air, as a result of which the fluorescent coating of the operational chamber is heated during four 200 s

intervals of alpha particle count accumulations. As a result, the efficiency of the coating increases, which leads to a noticeable rise in measurement errors. During measurements, the operational chamber of the radon activity sensor was insulated on the outside by polyurethane foam and periodically damped with water and the measuring device was shielded from direct sunlight.

Similarly, samples of atmospheric air were analyzed that partially equalized the measurement errors of radon in the soil and the atmosphere. The volumetric activity of radon in the atmosphere is substantially less than in the soil, usually falling to levels around tenths to units of becquerels per liter.

Taking into account the half-life of thoron, τ_{Tn} = 57 s, it was assumed that the number of α-decays at the first reading was additive and consisted of the bulk of the α-activity of radon, while the thoron decayed almost completely. For the next three 20 s counts, only the α-decay of radon in the working chamber of the device was discoverable. Such an assumption is fully justified since almost four half-lives of thoron fit the time interval of the first count, that is, the volume concentration of Tn in the working chamber of the measuring device naturally decreased by more than an order of magnitude.

The radon activity in a sample is calculated by averaging 2 to 4 counts. Accordingly, after averaging, the error in determining the volumetric activity of radon at each observational station decreases to about 17 %.

Following analysis of the measurements obtained over many years, one can say that the data sets on the volumetric activity of soil radon and atmospheric radon correlate to one another [35, 36]. There is no correlation of these parameters with the volumetric activity of atmospheric thoron. This is due to the minimal values of the volumetric activity of atmospheric thoron. Over the entire observation period, the volumetric activities of these radiogenic gases were comparable to one another only at a profile passing over a rock crushing zone (Pelagiada Farm, Stavropol Territory) (Figure 1.1.5). According to the drilling data, the surveyed area was located in the rock crushing zone.

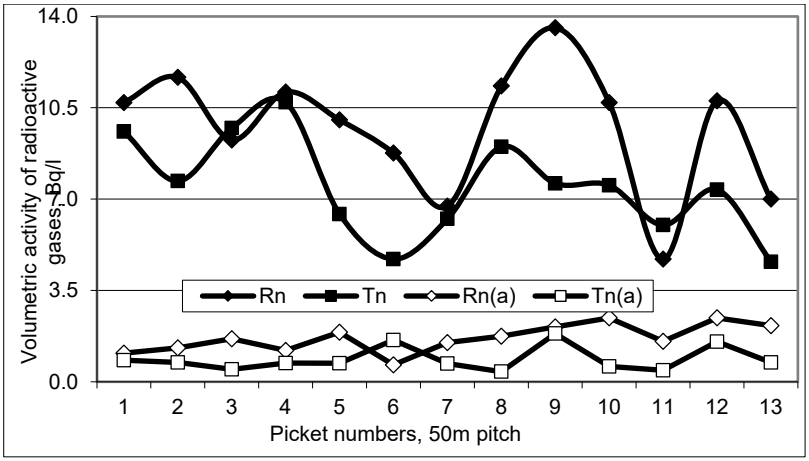

Figure 1.1.5: An example of comparable radon and thoron volumetric activities.

Before 2004, during fieldwork, one or two identical volumetric soil hydrogen concentration sensors, GVK G-01, designed and manufactured by the Moscow Engineering Physical Institute (MEPHI), were used as appropriate [37]. The principle of the sensor was based on variations in condenser capacitance, in which the permittivity of the gasket varied depending on hydrogen concentration in the working chamber of the measuring device.

The next modification of the measuring device, the hydrogen geophysical signaling device VSG-01, was designed for long-term continuous measurements of hydrogen concentrations in soil or atmospheric air [38]. Transfer of the measuring device to online recording caused some changes in the observation technique and the construction of the working chamber. In the original version, the sensor was designed for the natural flow of the soil or atmospheric air. To this end, the remote module with the sensitive element of the sensor was buried in the ground or placed in the investigated volume of the atmosphere. In the online mode, the working chamber of the remote module was sealed from direct air intake. The measurement cycle at the observation picket consisted of a series of procedures. First of all, the working chamber was pumped with atmospheric air, and the readings taken were assumed to be zeroed. Then, a sample of a tabulated volume of soil air—30 ml for the VSG-01 sensor—was introduced into the working chamber. The difference between the signal and the zero samples

was assumed to be due to the volumetric hydrogen concentration in the soil.

The measured volumetric hydrogen concentrations were in the range 0.1 to 50.0 ppm, with a relative error of about 10 % of the current background values. The transition to the volumetric concentration of hydrogen in the sample in ppm is implemented according to the calibration graph. In the range of 0.0 V to 1.5 V, the sensor division value (roughly) is 1 ppm—30 mV.

Since 2005, the complex has used next-generation measuring devices: VG-2B #18 & #19 gas detectors [39]. With the same operating parameters, the sensor has a 6–8 ml working chamber, rather than a 30 ml one, consumes less power, and is structurally better suited to field operation.

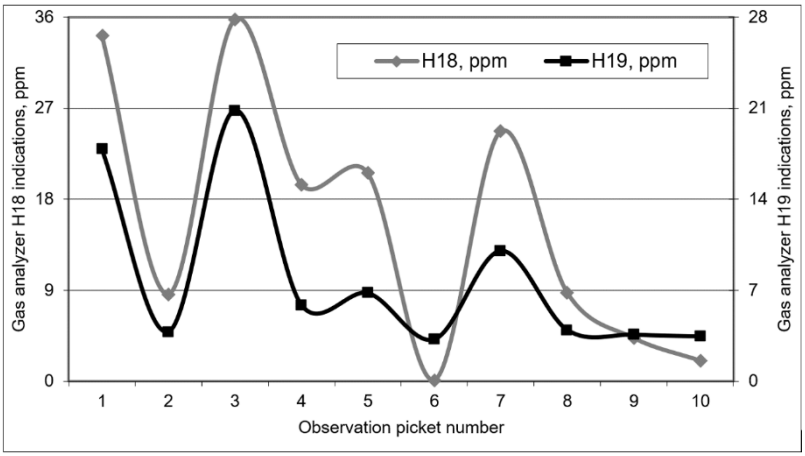

Figure 1.1.6: Verification results for the identity of hydrogen sensors VG-2B #18 & #19 before leaving for fieldwork in 2008.

In autumn 2006, in cooperation with the developer, a simultaneous sampling technique using two VG-2B sensors was improved. Sensitive elements of the instruments were introduced in the same working chamber of about 0.5 l. According to the laboratory calibration, a nonlinear transient function was introduced for each sensor with a confidence value of 0.99, which associates signals in [mV] with [ppm]: $H18_{ppm} = 0.0013(H18_{mV})^{1.589}$; $H19_{ppm} = 3.2178 \times \exp[0.0027(H19_{mV})]$. The results of the joint testing of the measuring devices are shown in Figure 1.1.6. In the latter version of

air sampling at the observation picket, only one sampling well was used. The selection was performed sequentially, through a 0.5 l volume of the hydrogen sensors in the working volume of the radon sensor.

The sensors of the atmospheric electric field Pole-2 and gradient allowed for absolute calibration at the installation site. This calibration was carried out daily before and after the start of operation.

A measuring device, RGA-01, for recording the volumetric activity of radon was calibrated at the All-Russian Research Institute of Physical and Technical Measurements and Radio Metering (VNIIFTRI) before and after fieldwork. The scatter of readings fit the error limits of the measuring device. A similar procedure was carried out for the hydrogen sensors at the Moscow Engineering and Physics Institute.

Checking of the operational stability of the aspiration capacitor unit was carried out at the site in the Moscow Region. Before and after the fieldwork and in fair weather conditions, the sensor was checked at eight fixed pickets of similar profile. Over the entire observation period, the correlation coefficient of the profile variations of polar conductivities did not descend below 0.7.

1.2. Model of the Relationships between Hydrogen, Methane, Radon, and Elements of Surface Atmospheric Electricity

The first experimental results illustrating the relationships between methane, hydrogen, radon, and the atmospheric electric field were obtained at the Alexandrovsky Structure of the Gomel Region in Belarus [40, 41]. Elevated concentrations of methane, hydrogen, and radon were recorded above an oil reservoir and the fault structure was, in turn, indicated by a decline in the atmospheric electric field, AEF.

In 1998, the same regularities were observed at the Kaluga Ring Structure [42]. On two profiles intersecting at the center of the structure, with a length of 20 km and 18 km, radon and hydrogen in the soil air and the atmospheric electric field were measured using a unified system of observation pickets (21 pickets and 19 pickets, respectively). At the same time, the soil air was sampled at eight pickets for subsequent quantitative analysis of hydrogen, nitrogen, carbon dioxide, methane, and their homologs in the laboratory.